Direct Observation of Heterogeneous Photochemistry on Aggregated Ag Nanocrystals Using Raman Spectroscopy: The Case of Photoinduced Degradation of Aromatic Amino Acids

Erik J. Bjerneld,† Fredrik Svedberg, Patrik Johansson, and Mikael Käll*

Department of Applied Physics, Chalmers University of Technology, SE-412 96 Göteborg, Sweden

Received: October 6, 2003; In Final Form: March 4, 2004

We show that aromatic amino acids on aggregated and immobilized Ag nanocrystals degrade upon laser illumination ($\lambda = 514.5$ nm). Surface-enhanced Raman scattering (SERS) data, using tyrosine as the precursor, point to a linear one-photon induced reaction. This interpretation is supported by ab initio calculations of tyrosine−Ag^+ complexes. Spectral fluctuations and bleaching-effects suggest that the observed SERS signal is due to a variety of chromophores that continuously form from aromatic precursors and eventually break down at the Ag surface. The final photoproduct is similar to amorphous carbon (AC) but the spectral details are determined by the precursor. We found that precoating the Ag particles with thiophenol inhibits photoinduced degradation of tyrosine in H_2O.

1. Introduction

Surface-enhanced Raman scattering (SERS) experiments using a microscope to illuminate a small number of immobilized Ag nanoparticles have allowed observations of hitherto hidden fluctuations in Raman spectra. Observations of SERS flickering and blinking,[1−6] photoinduced fluctuations,[7,8] and inhomogeneous broadening of Raman bands[1,9,10] have now been reported. The temporal and spectral SERS fluctuations, in combination with extremely low analyte concentrations, are evidence that single molecules were observed.[1−10]

We have reported that the broad SERS spectrum from aggregated Ag nanoparticles immersed in dense tyrosine solutions exhibits a remarkable inhomogeneous broadening.[1] The broad ensemble spectrum concealed a multitude of different single-molecule spectra that varied with time, each with a unique set of a few narrow Raman lines, signifying substantial disorder in the surface adsorbate population. Kudelski and Pettinger[9] and Moyer et al.[10] have reported similar broad spectra and spectral dynamics from amorphous carbon (AC) layers. The broad ensemble SERS spectrum we reported was very similar to the spectrum of AC, suggesting that the ensemble SERS spectrum came from an AC-like film rather than from isolated tyrosine−Ag complexes. We here report that the earlier SERS spectra[1] came from photoproducts very similar to AC. In this article, using aromatic amino acids and thiophenol as precursors, we show that micro-Raman spectroscopy permit investigations of heterogeneous photochemical reactions in the first surface layer on Ag nanoparticles. A similar SERS study of single-molecule chemistry of Rhodamine 6G has recently been reported by Emory and co-workers.[11]

In the seminal paper by Nitzan and Brus,[12] it was pointed out that the enhanced electromagnetic fields near metal nanoparticles, which give rise to SERS, should also enhance fluorescence and photochemistry. Indeed, surface-enhanced fluorescence and surface-enhanced photochemistry have been reported.[13−16] Moskovits and co-workers have in a series of papers examined photochemical effects using SERS.[17−23] Here, we are interested in the photochemical formation of amorphous carbon (AC) from aromatic precursors on a rough Ag surface. This reaction was first investigated by Goncher and Harris[14,15] and later by Wolkow and Moskovits.[17]

Although AC has been rather ubiquitous in SERS investigations,[24−26] the exact nature of the AC surface phase(s) is poorly understood and a number of terms have been used to describe it (e.g., amorphous graphite, carbonaceous groups, rafts, carbon chains, carbon clusters, nano-crystalline carbon, sheets, carbon networks, and carbon domains). Clearly, AC SERS spectra are very similar to those of amorphous graphite observed by Tuinstra and Koenig using ordinary Raman scattering,[27] indicating that graphite forms at the surface. However, the assignment of the broad spectrum to extended carbon chains has been questioned by Schwan et al. who showed that small clusters of condensed benzene rings in carbon films (cluster size below 20 Å) has a similar broad spectrum.[28] This experimental situation is similar to the measurements reported here, and previously,[1] since aromatic ring molecules are added in excess to aggregated Ag particles and a dense film should embed the inhomogeneous particle layer. Therefore, we use the term AC in its broadest sense, without specifying the structure further, at this point.

The first evidence, to our knowledge, of laser-induced AC formation on a metal surface is the report by Tsang et al. on the appearance of broad AC bands in SERS from benzoic acid monolayers on Ag.[26] The bands, were however, not observed when the power density was decreased from 10 to 0.5 W/cm^2 or when the sample was kept at low temperatures, which indicate thermal AC-formation. The authors noted that the carbon-like layer was created "at the expense of the benzoic acid monolayer" but did not discuss the mechanism further. As discussed before,[26] amorphous carbon is resonantly excited in a Raman measurement. Recent work has clarified this point and shown that dispersion effects in Raman spectra are due to resonant excitation of different parts of the AC structure at different wavelengths.[29]

The aromatic precursors used in this study absorb UV light only. Therefore, the two most reasonable photochemical reaction

* To whom correspondence should be addressed. E-mail: kall@fy.chalmers.se.

† Present address: Amersham Biosciences, Björkgatan 30, SE-751 84 Uppsala, Sweden.

10.1021/jp037004l CCC: $27.50
Published on Web 04/21/2004

pathways using visible laser light are either that the molecule forms a metal−molecule complex, which absorbs the visible radiation, or that the absorption is a multiphoton process. In the first reports on photodecomposition of aromatics on rough Ag surfaces, data indicated a surface-enhanced two-photon reaction.[15,17] Later works have shown that also one-photon surface-enhanced photochemistry occurs for some aromatic molecules.[20,21]

It was also reported that spacer layers, which displace the precursor from the surface, increased the rate of photochemistry.[15] An optimal surface distance for surface-enhanced photochemistry is expected because of competition between increasing nonradiative decay of photolabile excited states closer to the surface and the enhanced EM-fields decreasing in strength out from the surface.[12] Moskovits and co-workers later showed that the deposited surface layers led to interference effects in the SERS intensity, causing the observed distance dependence. Their measurements showed that the surface-enhanced photochemistry, which can be monitored by SERS, occurs directly at the surface.[17,18] It has furthermore been reported that overlayers protect polymers from photodecomposition, indicating photooxidation reactions.[30]

Photochemical decomposition on colloid surfaces has been observed for substituted benzenes that adsorb with the ring perpendicular to the silver surface.[19] In that work, thermal fragmentation of the particles at high irradiance was inferred from a decreased photodecomposition rate. The reported measurements were performed in solution, with particles diffusing in and out of the detection volume. In contrast, we have measured on immobilized particles. This leads to high accumulated photon doses and requires low irradiance for observing the kinetics of the photoinduced reactions. On the other hand, the lack of particle diffusion simplifies the analysis.

In this article, we demonstrate that the exquisite sensitivity of SERS can be used to monitor low-rate heterogeneous photochemical reactions, in particular surface-enhanced formation of AC from aromatic amino acids. Different aromatic amino acids all give very broad but different AC SERS spectra. This shows that the exact composition of the photoinduced AC film depends on the precursor. Using thiophenol as a self-assembled monolayer spacer, we show that the surface-enhanced photochemistry occurs in the first surface-layer. Furthermore, we show that the thiophenol layer alone also exhibits laser-induced growth of AC, although at a much slower rate than for the aromatic amino acids. This AC formation could be completely suppressed by immersing the particles in water, indicating additional laser-induced heating effects in air or a photochemical role of O_2. For long observation times and low irradiance, or short times and high irradiance, we observed a decrease in the AC−SERS intensity. This observation, together with the flickering SERS signal observed during AC growth, strongly indicates formation of transient chromophores that eventually bleach to nonresonant products. We suggest that the transient chromophores are *single* intermediate species in a highly heterogeneous photochemical reaction.

The results are discussed in relation to single-molecule SERS experiments and enhanced local EM fields. In this scenario, the photochemistry is localized to the nm-sized cavities between the aggregated Ag particles. Such sites can be expected to enhance the rate of photochemistry up to $\sim 10^5$ times (for an enhancement of the pumping intensity that is proportional to E^2). In this case, we expect the photoreactions to be diffusion-limited. We have observed that single-protein SERS spectra, from experiments using protein-induced aggregation of Ag particles, exhibit an AC-like background even at very low incident power,[31,32] which indicates surface-enhanced photochemistry also in these low-irradiance experiments.

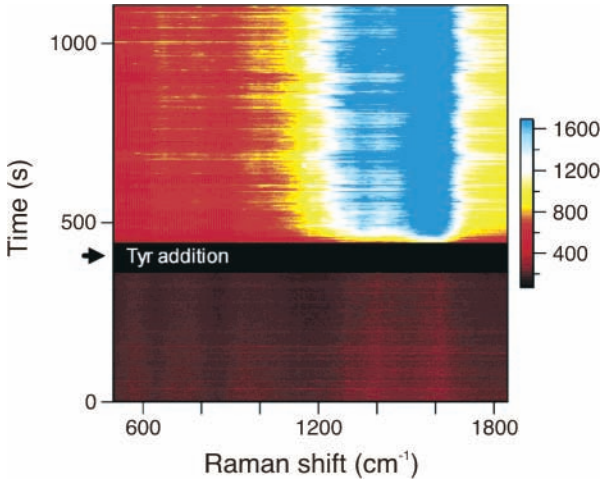

Figure 1. Laser-induced SERS spectra. Time-series of SERS spectra recorded before and after addition of tyrosine to immobilized, aggregated, 90-nm Ag particles immersed in H_2O. The addition of a high concentration ([Tyr] > 0.1 mM) Tyr solution is indicated by the arrow. The time-series show that citrate spectra before addition (bottom) are weak and stable. After addition, a delayed SERS intensity increase was observed. The initial SERS intensity increase was observed each time a new area of the sample was illuminated, which shows that the SERS intensity increase was laser-induced ($I = 2$ kW/cm^2, $\lambda = 514.5$ nm). The color scale-bar indicates SERS intensity.

2. Materials and Methods

The experimental setup and the materials have already been described in detail.[1] In short, we used the 514.5 nm line of an argon laser for excitation of Raman spectra and a Renishaw 2000 Raman microscope to record the spectra. The sample substrate consisted of layers of immobilized Ag particles with an average size of 90 nm. The particles were deposited on the surface by controlled evaporation of Ag sol droplets on a glass slide. Ring patterns consisting of dense layers of Ag particles form at the droplet edges. The particle substrates were then immersed in water and viewed with a water-immersion objective (60×) or air objectives (50× or 100×). The same objective was then used for illumination and collection of backscattered light. The laser focus of the immersion objective was estimated to have a diameter of ~ 1 μm. The macroscopic particle aggregates we measured from were always larger that the beam diameter, and we estimate that ~100 Ag particles were in the detection volume. All Raman measurements were performed on immobilized and aggregated particles.

To avoid contamination problems, we always checked the weak and stable citrate spectrum of the Ag particles in H_2O before adding the analyte to the particles, see Figure 1. We added the analyte in excess (typically 0.2 mM) to the particles with the laser light turned off. When the laser light was turned on, we recorded spectra as a function of time. The finite integration time was taken into account when fitting exponential functions to the SERS intensity growth curves.

The SERS measurements of aromatic amino acids were done on particles immersed in water. In some experiments, a Tyr solution was added to thiophenol-coated particles. Thiophenol-coated particles were prepared by incubation of immobilized and aggregated Ag particles in 10 mM thiophenol (benzenethiol) in ethanol for 4 h. The particles were then rinsed with ethanol

and water. Measurements on thiophenol alone were performed both in water and in air to investigate laser-induced heating effects.

3. Computational

The tyrosine molecule and a metal−molecule complex tyrosine−Ag^+ (with the Ag^+ ion at the carboxyl group of tyrosine[1]) were geometry optimized in the ground state by density functional theory (DFT) calculations using the hybrid functional B3LYP[33,34] and the standard 6-31+G* basis set. For Ag^+, the LanL2DZ pseudo-potential basis set was used.[35] For both systems, time-dependent DFT (TD-DFT) calculations were performed to obtain energies, wavelengths, and oscillator strengths for the ground to excited-state transitions. All calculations were made using the program package Gaussian 98.[36]

4. Results

A typical measurement is displayed in Figure 1. We first ensured that the immobilized Ag particles, immersed in H_2O, exhibited a stable citrate SERS spectrum (citrate comes from the particle synthesis). We then added tyrosine in the dark. Then the laser light was turned on, and spectra were recorded as a function of time. For aggregated particles, we observed a delayed SERS intensity increase upon illumination as shown in Figure 1. Furthermore, each time we investigated a new area on the Ag-particle substrate, we observed an increase of SERS intensity; that is, the initial increase of the SERS signal was independent of the waiting time between adsorption of tyrosine and start of illumination. This shows that the broad SERS spectrum was induced by the laser irradiation. In contrast, the same type of experiments performed on isolated Ag particles on APTMS did not show any laser-induced SERS signal.

To investigate whether the laser-induced SERS intensity increase was caused by a thermal or photochemical mechanism, we investigated the growth rate as a function of laser irradiance. The initial SERS intensity growth could be well described by a single-exponential function, as shown in Figure 2. We observed no threshold excitation irradiance for the laser induced SERS increase, see Figure 2. Such a threshold would be expected for a thermal process since the local temperature can be expressed as $T_{loc} = T_0 + kP$, where T_0 is the ambient temperature, k is a proportionality constant, and P is the power. Because the particles are immersed in an aqueous solution for cooling, and the incident power was as low as 100 nW (corresponding to an excitation irradiance of 6 W/cm^2), we conclude that thermal processes can be neglected and that the initial laser-induced SERS intensity increase is a true photoinduced phenomenon. The dependence of the time-constant on excitation irradiance can be well fitted by a linear function, as expected for a one-photon photoinduced process.

The rate of SERS increase showed large sample-to-sample variation, probably due to differences in aggregation state of the immobilized particles. The state of aggregation is a key parameter in SERS and slight differences in the sample preparation are expected to produce different SERS substrates. Therefore, the data in Figure 2 was measured from the same sample. Minor variations in the photochemical rate-constants were also observed for different sites on the same sample. The most striking SERS fluctuations, however, occurred during growth and even after the SERS intensity had reached its plateau value, as indicated by the arrow in Figure 2. Very long integration times (∼1000 s.) were required to average out these temporal SERS fluctuations. This observation of heterogeneous

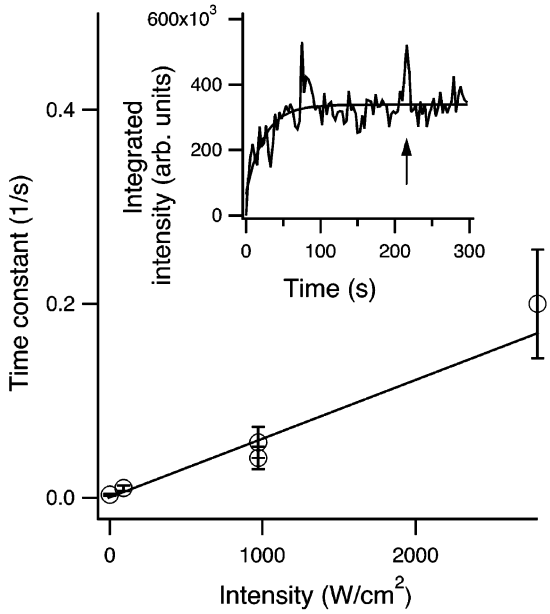

Figure 2. Initial SERS intensity increase is a photoinduced process. The inset shows the initial increase of SERS intensity over time. The spectral data were obtained at constant irradiance ($I = 1$ kW/cm^2) and collected from one sample consisting of large aggregates (larger than the detection area) of immobilized 90-nm Ag particles, in a 0.2 mM Tyr solution. The SERS increase could be well fitted by an single-exponential function, $i(t) \sim 1 - e^{-Ct}$ (error-bars were obtained from the fit). The SERS intensity fluctuates with time, even after saturation of the SERS intensity ($t > 100$ s), see for example the burst indicated by the arrow (the corresponding spectrum is shown in Figure 6). The figure shows how the time constant C varied with excitation intensity. No thresholds were observed, showing that the process is photoinduced. The data could be fitted well with a linear function $C = kI$, where k is a constant.

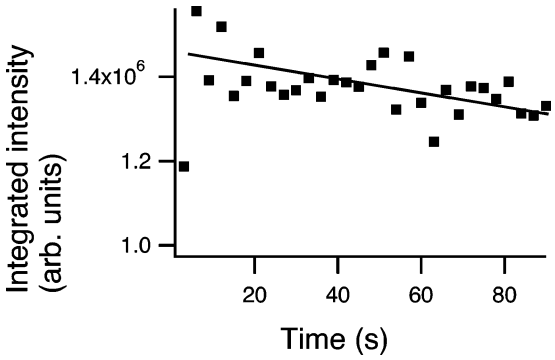

Figure 3. At high irradiance, or at low irradiance and long integration times, the SERS intensity of the AC photoproduct decreased with time. The experimental conditions were the same as in Figure 2, but the irradiance was 9 kW/cm^2. The line is a guide for the eye.

dynamics shows that the SERS signal comes from a very small number of contributing species.

At high laser irradiance, or for long observation times and low irradiance, a slow decay in SERS intensity over time was observed, as shown in Figure 3. This indicates that the Raman active species slowly bleach away upon irradiation. At high irradiance, the particles remained immobilized and appeared to be intact by inspection in the microscope. Furthermore, at this irradiance level, we could still measure SERS from thiophenol, see below, which rules out particle degradation. The finite time required to record a spectrum (∼1 s) prevented observation of the initial SERS intensity growth at high laser fluence. In fact, when particles that had been exposed to Tyr were illuminated in air, the initial SERS intensity increase was so fast that it

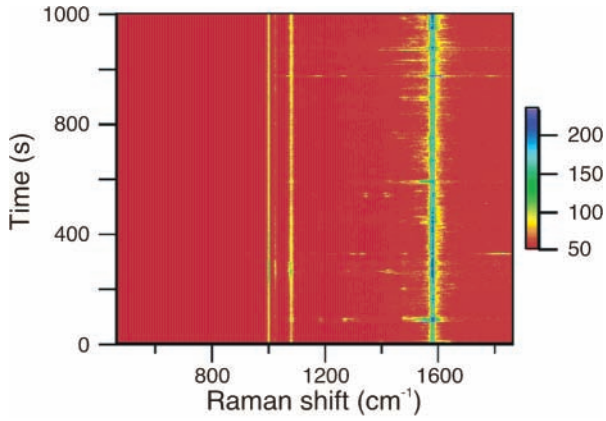

Figure 4. Ag surface plays an important role in the heterogeneous photochemical transformation of aromatic molecules to AC. The aggregated Ag nanoparticles were precoated with thiophenol. Despite a high concentration (0.4 mM) of tyrosine in the surrounding solution and high irradiance (9 kW/cm^2), there is no photoinduced AC spectra. The complete inhibition of the photochemical conversion of tyrosine to AC by the thiophenol coating indicates that the bare Ag surface is required for AC formation. The color scale-bar indicates Raman intensity.

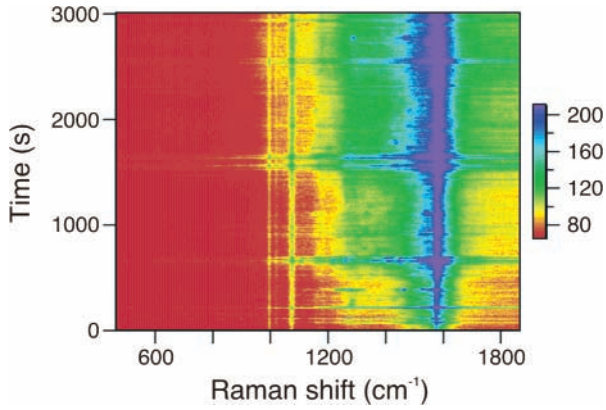

Figure 5. AC formation in air from SERS substrates precoated with thiophenol. The time series show that, at an irradiance of 4 kW/cm^2, AC forms despite the fact that thiophenol is covalently bound to the Ag surface. However, the AC formation is completely suppressed by immersing the particle-substrate in H_2O, see Figure 4, which indicates that the AC-formation in this case is caused by laser-induced heating. The colors indicate Raman intensity.

could not be detected, i.e., only a slow decrease in intensity was observed over time.

To understand the photochemical mechanism for amino acid degradation further, we performed experiments in which the Ag-particle layer had been precoated with a self-assembled monolayer (SAM) of thiophenol. The surrounding solution in the experiment displayed in Figure 4 is the same dense Tyr solution that normally gives rise to intense AC-like spectra. However, in this case, only the distinct SERS spectrum of thiophenol is observed, despite an excitation intensity of 9 kW/cm^2. Thus, the thiophenol monolayer inhibits photochemical degradation of the tyrosine precursor at the surface. This indicates that binding to the Ag surface is required for efficient photochemical transformation of the aromatic molecules.

We also investigated the time evolution of thiophenol SERS for Ag particles in air. The time series in Figure 5 shows that in that case there is a gradual increase of AC-like SERS bands with illumination time. However, the growth is much slower than for tyrosine at the corresponding irradiance. Thus, for both tyrosine and thiophenol, the results show that the photochemical

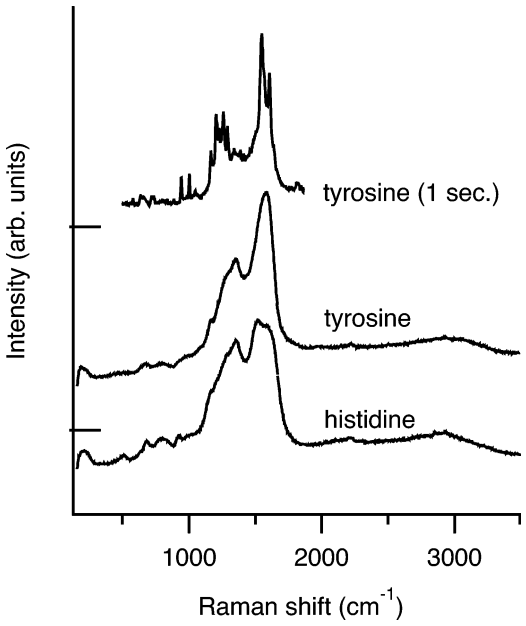

Figure 6. Nature of the photoproduct depends on the precursor. The photoproduct SERS spectra from immobilized particles immersed in histidine and tyrosine excess (0.5 mM) are compared. The broad spectra are assigned to an amorphous carbon (AC) like film. However, the two spectra differ significantly, which shows that the exact composition of the AC-like photoproduct is determined by the aromatic precursor. To illustrate the effect of using short integration times, we show the "burst-spectrum" from the time-series in Figure 2, for comparison with the ensemble-case. Bars indicate offsets.

degradation of aromatic precursors is much more efficient in air than in water. This may indicate an additional heating effect in air or a role of oxygen. Irrespective of the surrounding medium, tyrosine degrades much faster than thiophenol, which completely inhibits tyrosine degradation in water. This indicates that some form of direct bond between the precursor and the Ag is a requirement for photochemical degradation and that the nature of this bond greatly influence the speed of the reaction. We note that thiophenol is covalently bound to the Ag surface, as evidenced from spectra,[1] whereas tyrosine probably has a weaker and more unspecific interaction with the Ag-surface.

As mentioned in the Introduction, we interpret the photoproduct SERS spectra in terms of an AC-like film that forms directly on the Ag surface. To further study the nature of the photoproduct, we measured SERS using several aromatic amino acids (tyrosine, phenylalanine, tryptophan, and histidine) as photochemical precursors. The SERS substrates used here were prepared according to a recently developed methodology.[37] Although all photoinduced spectra share a common similarity to AC, indicating that all four molecules photoconvert in a similar fashion, there are clear spectral differences between the four different amino acids. The largest difference was observed for histidine compared to the other aromatic amino acids, see Figure 6. This is expected because histidine contains a five-atom ring compared to the benzene-rings of the other molecules. Thus, although the photoproduct is obviously similar to amorphous carbon, its detailed structure depends on the precursor.

5. Discussions

The fluctuations in amino acid SERS, discussed in detail previously[1] together with the results presented here show that we are directly observing a heterogeneous photochemical reaction. The heterogeneity is fascinating in itself, but the

multitude of different spectra and the intricate spectral dynamics obviously complicates the assignment of spectra to specific photoproducts. Normal Raman spectra of the aromatic amino acids only exhibits a small number of Raman lines in the 1400−1700 cm^{-1} region, whereas ensemble averaged SERS produce a 400 cm^{-1} continuum of nonresolved Raman bands. Similar broad spectra have been observed by Nabiev and co-workers.[38,39] In our first report on this phenomenon, we argued that tyrosine in different orientations at the surface, together with deprotonated and radical forms of tyrosine, could generate sufficient variation in the adsorbate population to explain the inhomogeneous broadening.[1] However, since the broad ensemble SERS spectrum is photoinduced, this is obviously not the case. In the previous SERS literature, we have found some reported spectra of aromatic amino acids that most probably also come from photoproducts.[38,39] Kim and co-workers observed that circulation of the Ag sol could be used to avoid laser-induced effects. Although some broad spectral features in the 1300−1600 cm^{-1} region indicate photoproduct contributions, their approach apparently allowed for successful recording of ensemble Tyr SERS spectra.[40,41] However, we aimed at detecting single molecules of aromatic amino acids and therefore aggregated the Ag particles in order to induce a large electromagnetic enhancement effect. We further investigated immobilized Ag particles, which consequently led to high accumulated photon doses. An important point is that the very sites that are monitored in single molecule SERS, the so-called "hot spots", are sites with greatly enhanced local optical fields. These fields will enhance any photochemical process. Thus, the surface sites where photochemistry is most probable are also the sites observed in these ultra-sensitive SERS measurements. Using immobilized and aggregated 90-nm Ag particles to obtain highly efficient "hot spots" will consequently also provide high-yield photochemistry sites. Therefore, in retrospect, the surface-enhanced photochemistry is not surprising. In addition, we also tried to use single immobilized Ag particles for SERS measurements, without detecting any photochemical process or SERS signal. This is not surprising, as single particles are, in general, not expected to contain sites with high enough surface enhancement for single molecule SERS.[42]

We now turn to the mechanism of the photochemical reaction. The aromatic precursors do not absorb light in the visible, and it is therefore likely that the first reaction step is surface-enhanced absorption of light by metal-molecule complexes. Evidence for such a scenario is the experimental observation that a thiophenol spacer layer inhibits the photochemistry and that the rate of formation depends linearly on irradiance. In addition, it has been reported that phenylalanine forms a complex with Ag colloids that absorbs light in the visible.[39] This also indicates that absorption of light by a metal-molecule complex is the first step in the photochemical degradation of aromatic molecules.

To assess this scenario further, we computed the ground and excited-state properties of both pure tyrosine and a metal-molecule complex. The metal surface is modeled as a single silver ion in accordance with earlier studies.[43−45] As seen in Figure 7, both structures have very similar HOMOs but very different LUMOs, resulting in a much smaller HOMO−LUMO energy gap for the metal-molecule complex. From the TD-DFT calculations, we obtain S_0-S_1 excitation wavelengths (oscillator strengths) of 253 nm ($f = 0.032$) and 511 nm ($f = 0.015$), respectively, for the pure tyrosine and the metal-molecule complex. Both have the character of HOMO to LUMO transitions. The next excitation for the metal-molecule complex has a higher energy (3.35 eV) and a lower oscillator strength: $f = 0.002$. Thus, with an experimental laser wavelength of 514.5 nm, we are very close to the computed absorption maxima of the first ground-to-excited-state transition of the metal-molecule complex, whereas a tyrosine molecule should not be able to absorb.

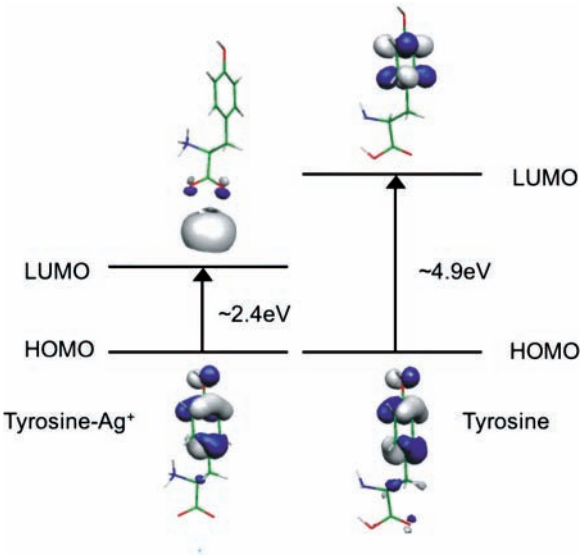

Figure 7. Schematic diagram of the lowest energy excitations of Tyr and the effect of Ag complexation.

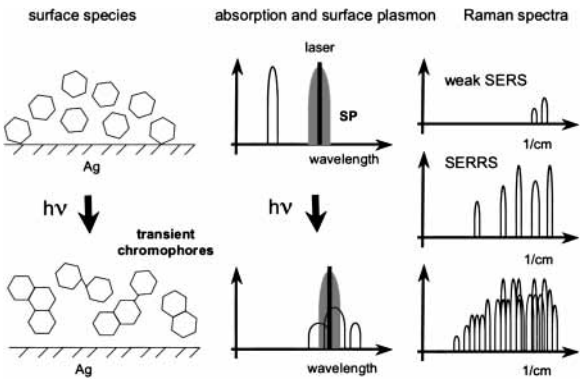

Figure 8. Heterogeneous photochemistry gives rise to inhomogeneous broadening of SERS bands. Nonresonant aromatic molecules (represented by the benzene rings) form complexes with the Ag surface and undergo photochemical transformation into an AC film. In the process, a multitude of different transient chromophores form at low rate. Nonresonant products are formed when the transient chromophores photobleach and are not detected by SERS measurements. This process gives rise to temporal and spectral fluctuations of SERS spectra, which explains the inhomogeneous broadening, and leads to a slow decay of the overall SERS intensity.

Based on the results presented here and the previous observations,[1] we propose the following general interpretation of photochemical effects and inhomogeneous broadening in SERS of aromatic species, as illustrated schematically in Figure 8. Nonresonant aromatic molecules, like thiophenol or amino acids, bind to the Ag surface, which enables photoinduced molecule-metal charge transfer, as in Figure 7. Depending on the strength and type of the metal-molecule bond, there is a certain possibility for chemical transformation/degradation in the excited state. In particular, two or more photolabile species may react to form larger chromophoric entities. Such species may then give rise to surface-enhanced resonance Raman scattering (SERRS). We note that the SERRS cross-section for chromophores, like Rhodamine 6G, are often orders of mag-

nitude larger than the ordinary SERS cross-section of nonresonant aromatic species, like thiophenol. Consequently, even a small fraction of photoinduced chromophoric species may dominate a SERS spectrum. The photoinduced chromophores eventually bleach or react to form larger nonresonant species, which leads to an overall decrease of the Raman intensity over time.

In the case of tyrosine, the spectral variation indicates that a large variety of different intermediate chromophores form, which implies that the photochemical reaction pathway is highly branched and that many reactions may proceed in parallel at different surface sites. We previously observed that many of the transient SERS spectra were similar to resonance Raman spectra of phenoxyl radicals.[1] It is possible that such radical species are stabilized by the Ag surface and initiate a radical-chain reaction upon absorption of light, i.e., a photoinduced polymerization reaction. We note that polymerization of aromatic rings has previously been reported to lead to broadening of SERS bands and shifts in peak positions of aromatic ring vibrations.[46,47]

It is clear that a heterogeneous formation of resonant intermediates at low rate would explain both the spectral and temporal fluctuations in tyrosine SERS spectra. The fact that the temporal ensemble averaged SERS spectra differ between different aromatic amino acids then implies that we observe different dynamic structures en route to the final structure.

In this scenario, the same photoinduced bleaching effect is involved in both the SERS fluctuations during growth and the final decrease of the overall SERS intensity. Therefore, the fluctuations in SERS intensity during the growth of SERS intensity are also expected to be photoinduced. This has been shown to be the case for R6G by Weiss and Haran.[7] Recent observations of photoinduced fluctuations in SERS measurements on both R6G and cytochrome *c* have also been made by Suh et al.[8] The data reported by Moskovits et al. (Figures 6 and 8)[22] indicates that this holds also for other surface-enhanced photochemical reactions. Interestingly, Kudelski and Pettinger found that the fluctuations in AC−SERS could only be observed if oxygen was present, suggesting a photooxidation process.[9] Similar results for hp-DNA were obtained by Etchegoin et al.[48] This indicates that the relation between SERS fluctuations and an oxygen-rich atmosphere is a general effect. Recent low-temperature SERS measurements of R6G display some discrepancies. Results from Anger et al. show significant blinking of the SERS signal at 77 K, which suggests a nonthermal mechanism.[49] In contrast, Futamata et al. report that blinking is suppressed at the same temperature and argue that blinking is due to thermal diffusion of molecules at the surface.[50] However, the presence of oxygen in the corresponding room-temperature measurements in the latter case is uncertain.

Although the surface-enhanced photochemistry reported here is fascinating in terms of the multitude of different transient species and the long time-scales involved in the spectral dynamics, it is an undesirable side effect in many SERS studies. In particular, single-molecule SERS, which is believed to rely on "hot sites" with ultrahigh photonic fields, is extra susceptible to photochemical reactions. For example, in single-protein SERS studies at very low irradiance, we have observed an AC-like background that most probably is photoinduced.[31,32]

A way to circumvent this problem is to excite SERS off-resonance, using NIR illumination, as reported by Kneipp and co-workers.[51] For resonance SERS investigations of single-molecules, it is possible to immerse the particles in water to avoid laser-induced heating of the sample and to overcoat the surface to avoid photooxidation.[30] A monolayer coating, like the thiophenol reported here, protects the analyte from photochemical reactions at the surface but will also result in a decreased SERS enhancement.

Finally, we note that the local EM-fields at "hot spots" are very difficult to measure directly. However, it should be possible to measure the photochemical cross-sections and get a new observable parameter of the local EM field at the surface.

Acknowledgment. The authors thank A. Otto for stimulating discussions. This work has been supported by the Swedish Foundation for Strategic Research and the Swedish Research Council.

References and Notes

(1) Bjerneld, E. J.; Johansson, P.; Käll, M. *Single Mol.* **2000**, *1*, 239.
(2) Nie, S. M.; Emery, S. R. *Science* **1997**, *275*, 1102.
(3) Krug, J. T.; Wang, G. D.; Emory, S. R.; Nie, S. M. *J. Am. Chem. Soc.* **1999**, *121*, 9208.
(4) Bosnick, K. A.; Jiang, J.; Brus, L. E. *J. Phys. Chem. B* **2002**, *106*, 8096.
(5) Bizzarri, A. R.; Cannistraro, S. *Chem. Phys.* **2003**, *290*, 297.
(6) Habuchi, S.; Cotlet, M.; Gronheid, R.; Dirix, G.; Michiels, J.; Vanderleyden, J.; De Schryver, F. C.; Hofkens, J. *J. Am. Chem. Soc.* **2003**, *125*, 8446.
(7) Weiss, A.; Haran, G. *J. Phys. Chem. B* **2001**, *105*, 12348.
(8) Suh, Y. D.; Schenter, G. K.; Zhu, L. Y.; Lu, H. P. *Ultramicroscopy* **2003**, *97*, 89.
(9) Kudelski, A.; Pettinger, B. *Chem. Phys. Lett.* **2000**, *321*, 356.
(10) Moyer, P. J.; Schmidt, J.; Eng, L. M.; Meixner, A. J. *J. Am. Chem. Soc.* **2000**, *122*, 5409.
(11) Emory, S. R.; Ambrose, W. P.; Goodwin, P. M.; Keller, R. A. *Proc. SPIE* **2001**, *4258*, 63.
(12) Nitzan, A.; Brus, L. E. *J. Chem. Phys.* **1981**, *75*, 2205.
(13) Wokaun, A.; Lutz, H. P.; King, A. P.; Wild, U. P.; Ernst, R. R. *J. Chem. Phys.* **1983**, *79*, 509.
(14) Goncher, G. M.; Harris, C. B. *J. Chem. Phys.* **1982**, *77*, 3767.
(15) Goncher, G. M.; Parsons, C. A.; Harris, C. B. *J. Phys. Chem.* **1984**, *88*, 4200.
(16) Chen, C. J.; Osgood, R. M. *Phys. Rev. Lett.* **1983**, *50*, 1705.
(17) Wolkow, R. A.; Moskovits, M. *J. Chem. Phys.* **1987**, *87*, 5858.
(18) Blue, D.; Helwig, K.; Moskovits, M.; Wolkow, R. *J. Chem. Phys.* **1990**, *92*, 4600.
(19) Suh, J. S.; Moskovits, M.; Shakhesemampour, J. *J. Phys. Chem.* **1993**, *97*, 1678.
(20) Suh, J. S.; Jang, N. H.; Jeong, D. H.; Moskovits, M. *J. Phys. Chem.* **1996**, *100*, 805.
(21) Jang, N. H.; Suh, J. S.; Moskovits, M. *J. Phys. Chem. B* **1997**, *101*, 8279.
(22) Jeong, D. H.; Suh, J. S.; Moskovits, M. *J. Phys. Chem. B* **2000**, *104*, 7462.
(23) Jeong, D. H.; Suh, J. S.; Moskovits, M. *J. Raman Spectrosc.* **2001**, *32*, 1026.
(24) Otto, A. *Surf. Sci.* **1978**, *75*, L392.
(25) Mahoney, M. R.; Howard, M. W.; Cooney, R. P. *Chem. Phys. Lett.* **1980**, *71*, 59.
(26) Tsang, J. C.; Demuth, J. E.; Sanda, P. N.; Kirtley, J. R. *Chem. Phys. Lett.* **1980**, *76*, 54.
(27) Tuinstra, F.; Koenig, J. L. *J. Chem. Phys.* **1970**, *53*, 1126.
(28) Schwan, J.; Ulrich, S.; Batori, V.; Ehrhardt, H.; Silva, S. R. P. *J. Appl. Phys.* **1996**, *80*, 440.
(29) Ferrari, A. C.; Robertson, J. *Phys. Rev. B* **2001**, *6407*.
(30) Venkatachalam, R. S.; Boerio, F. J.; Roth, P. G.; Tsai, W. H. *J. Polym. Sci. Part B−Polym. Phys.* **1988**, *26*, 2447.
(31) Xu, H. X.; Bjerneld, E. J.; Käll, M.; Börjesson, L. *Phys. Rev. Lett.* **1999**, *83*, 4357.
(32) Bjerneld, E. J.; Földes-Papp, Z.; Käll, M.; Rigler, R. *J. Phys. Chem. B* **2002**, *106*, 1213.
(33) Becke, A. D. *J. Chem. Phys.* **1993**, *98*, 5648.
(34) Lee, C. T.; Yang, W. T.; Parr, R. G. *Phys. Rev. B* **1988**, *37*, 785.
(35) Hay, P. J.; Wadt, W. R. *J. Chem. Phys.* **1985**, *82*, 270.
(36) Frisch, M. J.; Trucks, G. W.; Schlegel, H. B.; Scuseria, G. E.; Robb, M. A.; Cheeseman, J. R.; Zakrzewski, V. G.; Montgomery, J. A., Jr.; Stratmann, R. E.; Burant, J. C.; Dapprich, S.; Millam, J. M.; Daniels, A. D.; Kudin, K. N.; Strain, M. C.; Farkas, O.; Tomasi, J.; Barone, V.; Cossi, M.; Cammi, R.; Mennucci, B.; Pomelli, C.; Adamo, C.; Clifford, S.; Ochterski, J.; Petersson, G. A.; Ayala, P. Y.; Cui, Q.; Morokuma, K.; Malick, D. K.; Rabuck, A. D.; Raghavachari, K.; Foresman, J. B.; Cioslowski, J.; Ortiz, J. V.; Stefanov, B. B.; Liu, G.; Liashenko, A.; Piskorz, P.; Komaromi,

I.; Gomperts, R.; Martin, R. L.; Fox, D. J.; Keith, T.; Al-Laham, M. A.; Peng, C. Y.; Nanayakkara, A.; Gonzalez, C.; Challacombe, M.; Gill, P. M. W.; Johnson, B. G.; Chen, W.; Wong, M. W.; Andres, J. L.; Head-Gordon, M.; Replogle, E. S.; Pople, J. A. *Gaussian 98*, revision A.9; Gaussian, Inc.: Pittsburgh, PA, 1998.

(37) Bjerneld, E. J.; Murty, K.; Prikulis, J.; Käll, M. *ChemPhysChem* **2002**, *3*, 116.

(38) Chumanov, G. D.; Efremov, R. G.; Nabiev, I. R. *J. Raman Spectrosc.* **1990**, *21*, 43.

(39) Nabiev, I. R.; Savchenko, V. A.; Efremov, E. S. *J. Raman Spectrosc.* **1983**, *14*, 375.

(40) Lee, H. I.; Kim, M. S.; Suh, S. W. *Bull. Korean Chem. Soc.* **1988**, *9*, 218.

(41) Kim, S. K.; Kim, M. S.; Suh, S. W. *J. Raman Spectrosc.* **1987**, *18*, 171.

(42) Xu, H. X.; Aizpurua, J.; Kall, M.; Apell, P. *Phys. Rev. E* **2000**, *62*, 4318.

(43) Wu, D. Y.; Ren, B.; Jiang, Y. X.; Xu, X.; Tian, Z. Q. *J. Phys. Chem. A* **2002**, *106*, 9042.

(44) Giese, B.; McNaughton, D. *J. Phys. Chem. B* **2002**, *106*, 101.

(45) Vivoni, A.; Birke, R. L.; Foucault, R.; Lombardi, J. R. *J. Phys. Chem. B* **2003**, *107*, 5547.

(46) Tashiro, K.; Matsushima, K.; Kobayashi, M. *J. Phys. Chem.* **1990**, *94*, 3197.

(47) Shirai, E.; Urai, Y.; Itoh, K. *J. Phys. Chem. B* **1998**, *102*, 3765.

(48) Etchegoin, P.; Liem, H.; Maher, R. C.; Cohen, L. F.; Brown, R. J. C.; Hartigan, H.; Milton, M. J. T.; Gallop, J. C. *Chem. Phys. Lett.* **2002**, *366*, 115.

(49) Anger, P.; Feltz, A.; Berghaus, T.; Meixner, A. J. *J. Microsc.-Oxf.* **2003**, *209*, 162.

(50) Futamata, M.; Maruyama, Y.; Ishikawa, M. *J. Phys. Chem. B* **2003**, *107*, 7607.

(51) Kneipp, K.; Wang, Y.; Kneipp, H.; Perelman, L. T.; Itzkan, I.; Dasari, R.; Feld, M. S. *Phys. Rev. Lett.* **1997**, *78*, 1667.